# Technical Note
# Bubble size in a forced circulation loop reactor

Ali Fadavi[1]*, Yusuf Chisti[2] and Ladislav Chriaštel[3]

[1]*Department of Farm Machinery, Faculty of Agricultural Engineering, Ilam University, P.O. Box 69315-51, Ilam, Iran*
[2]*Institute of Technology and Engineering, Massey University, Private Bag 11 222, Palmerston North, New Zealand*
[3]*Faculty of Mechanical Engineering, Slovak University of Technology, Nám Slobody 17, 812 31 Bratislava, Slovakia*

**Abstract**

**BACKGROUND: The bubble size distribution in gas-liquid reactors influences gas holdup, residence time distribution, and gas-liquid interfacial area for mass transfer. This work reports on the effects of independently varied gas and liquid flow rates on steady-state bubble size distributions in a new design of forced circulation loop reactor operated with an air–water system. The reactor consisted of a cylindrical vessel (∼26 L nominal volume, gas-free aspect ratio ≈6, downcomer-to-riser cross-sectional area ratio of 0.493) with a concentric draft tube and an annular riser zone. Both gas and liquid were in forced flow through a sparger that had been designed for minimizing the bubble size.**

**RESULTS: Photographically measured bubble size distributions in the riser zone could be approximated as normal distributions for the combinations of gas and liquid flow rates used. This contrasted with other kinds of size distributions (e.g. bimodal, Gaussian) that have been reported for other types of gas-liquid reactors. Most of the bubbles were in the 3 to 5 mm diameter range. At any fixed low value of aeration rate ($\leq 1.8 \times 10^{-4}\,m^3s^{-1}$), increase in the liquid flow rate caused earlier detachment of bubbles from the sparger holes to reduce the Sauter mean bubble size in the riser region.**

**CONCLUSION: Unlike in conventional bubble columns where bimodal and Gaussian bubble size distributions have been reported, a normal bubble size distribution is attained in forced circulation loop reactors with an air–water system over the entire range of operation.**


**Keywords:** bubble size; forced circulation loop reactor; jet loop reactor; airlift bioreactor; mass transfer; gas holdup

## INTRODUCTION

Gas–liquid multiphasic systems are widely used as bioreactors, chemical reactors and mass transfer devices.[1–3] A knowledge of the bubble size and size distribution is essential for improved understanding of hydrodynamic and mass transfer characteristics of gas–liquid systems.

In most gas–liquid contacting devices, bubbles are usually generated by passing air or other gas through a perforated pipe or plate type of sparger. In strongly noncoalescing liquids such as aqueous solutions of salt and alcohols, the bubble size generated at the sparger persists in the fluid.[4,5] In coalescing systems, however, the prevailing bubble size in the dispersion is controlled not by the initial bubble size produced by the sparger, but by an equilibrium between the bubble coalescence and breakage.[1,2] In relatively coalescing fluids, for identical values of the specific power input, the Sauter mean bubble diameter in airlift reactors tends to be smaller than in bubble columns because the rapid circulatory flow of liquid in airlift reactors helps to break up gas bubbles.[1,6] In airlift reactors, the size of the bubbles impact on the design of the gas–liquid separator zone.[7] Here we report on the effects of gas and liquid flow rates on bubble size distribution in a new design of forced circulation loop reactor.[8,9]

## MATERIALS AND METHODS

Experiments were performed in a forced circulation internal loop reactor of 26 L nominal volume (16.3 L working volume).[9] The reactor consisted of a cylindrical vessel that was divided into riser and downcomer zones by insertion of a concentric draft-tube (Fig. 1). Air was sparged through a gas–liquid

* Correspondence to: Ali Fadavi, Department of Farm Machinery, Faculty of Agricultural Engineering, Ilam University, P.O. Box 69315-51, Ilam, Iran
E-mail: a_fadavi@yahoo.com
(*Received 1 May 2007; revised version received 18 June 2007; accepted 26 June 2007*)
Published online 14 September 2007; DOI: 10.1002/jctb.1766

sparger, as shown in Fig. 1. The sparger had separate inlets for gas and liquid. The liquid passed through a static mixer (*3*, Fig. 1) that induced a swirling motion. Gas was injected through four holes (*6*, Fig. 1) of 1 mm diameter located in the conical zone of the sparger such that the swirling liquid sheared the bubbles off the sparger holes as they formed. The size of bubbles at detachment depended on the flow rates of the gas and liquid. Combinations of low gas flow rates and high liquid flow rates, produced small bubbles. All experiments were carried out with air and water at $20 \pm 1\,^{\circ}\mathrm{C}$. Liquid circulation within the reactor vessel was generated by a combination of mechanical pumping and airlift action as discussed elsewhere.[9] Geometric details of the reactor are shown in Table 1.

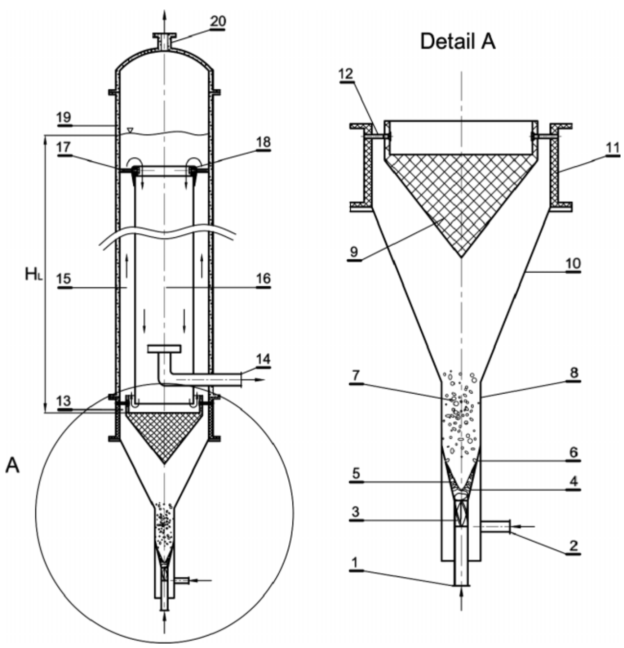


**Figure 1.** Details of the reactor: 1) liquid inlet; 2) gas inlet; 3) static mixer; 4) gas sparger; 5) conical liquid input zone; 6) orifice; 7) two-phase mixture; 8) mixing tube; 9) guiding cone; 10) diffuser; 11) support; 12) screw; 13) riser venturi entrance; 14) liquid outlet; 15) riser; 16) downcomer; 17) screw; 18) draft-tube support; 19) reactor vessel; 20) gas outlet.

**Table 1.** Reactor geometry and operational parameters

| Description | Value |
|---|---|
| Bioreactor diameter (m) | 0.1484 |
| Unaerated liquid height (m) | 0.914 |
| Liquid height above draft-tube (m) | 0.032 |
| Working volume × $10^2$ ($\mathrm{m}^3$) | 1.625 |
| Downcomer-to-riser cross-sectional area ratio (–) | 0.493 |
| Draft-tube length (m) | 0.865 |
| Inner diameter of draft-tube (m) | 0.083 |
| Static mixer | 20 mm length, 45° inclination angle |
| Mixing tube length (m) | 0.124 |

The dimensions of the bubbles were measured photographically. Images were taken near the wall of the column at the location that was closest to the camera that pointed at the centerline of the reactor. This minimized image distortion. A minimum of 60 bubble images were sampled at each hydrodynamic steady state. Lengths of the major and minor axes of the projected images of ellipsoidal bubbles were measured manually using the AutoCAD 2000 software. The diameter $d_B$ of the volume-equivalent sphere for the ellipsoidal bubbles was calculated as follows:

$$d_B = \left(x^2 y\right)^{1/3} \tag{1}$$

where $x$ and $y$ are the lengths of the major and minor axes of the ellipsoid in the two-dimensional projection, respectively. The bubble size distribution was characterized by Sauter mean diameter $d_{BS}$, or the total volume of the bubbles divided by the total gas–liquid interfacial area.[1,10]

## RESULTS AND DISCUSSION

The average bubble size reduced as the liquid flow rate increased. This was because at any fixed aeration rate, increasing flow rate of liquid increased turbulence and, therefore, turbulence associated bubble breakup was enhanced. Furthermore, a forced flow of liquid reduced bubble–bubble encounters that occur as a consequence of radial movement of bubbles. This in turn reduced bubble coalescence. A similar effect is known to occur in airlift reactors where the induced flow of liquid breaks up bubbles, reduces bubble–bubble interactions and postpones the onset of heterogeneous flow regime to higher values of aeration rate in comparison with conventional bubble columns operated at equal values of specific power input.[2,11] Similarly, in the bubble flow regime in conventional bubble columns, an increasing aeration rate is known to reduce average bubble size[12] because of increasing specific energy input and, therefore, increased turbulence.

Bubble size distributions for eight different combinations of gas and liquid flow rates are shown in Fig. 2. These distributions are for forced liquid flow rate values of $1\,\mathrm{m}^3\,\mathrm{h}^{-1}$ (left column, Fig. 2) and $2\,\mathrm{m}^3\,\mathrm{h}^{-1}$ (right column, Fig. 2). In each case, size distributions are shown for increasing values of aeration rate. Solid lines indicate best fit normal distribution curves. The results suggest that normal distribution satisfactorily approximates the observed bubble size distributions for the entire range of operating flow rates used.

In comparison with bubble columns, the existence of a normal size distribution in the riser zone of a forced flow loop reactor is different. Data in Fig. 2 are for a bubble flow regime, although in the absence of forced circulation some of the high aeration rate values would normally produce heterogeneous flow in the same reactor.[9] In bubble columns operated in heterogeneous flow, bimodal distributions of bubble



*J Chem Technol Biotechnol* **83**:105–108 (2008)
DOI: 10.1002/jctb

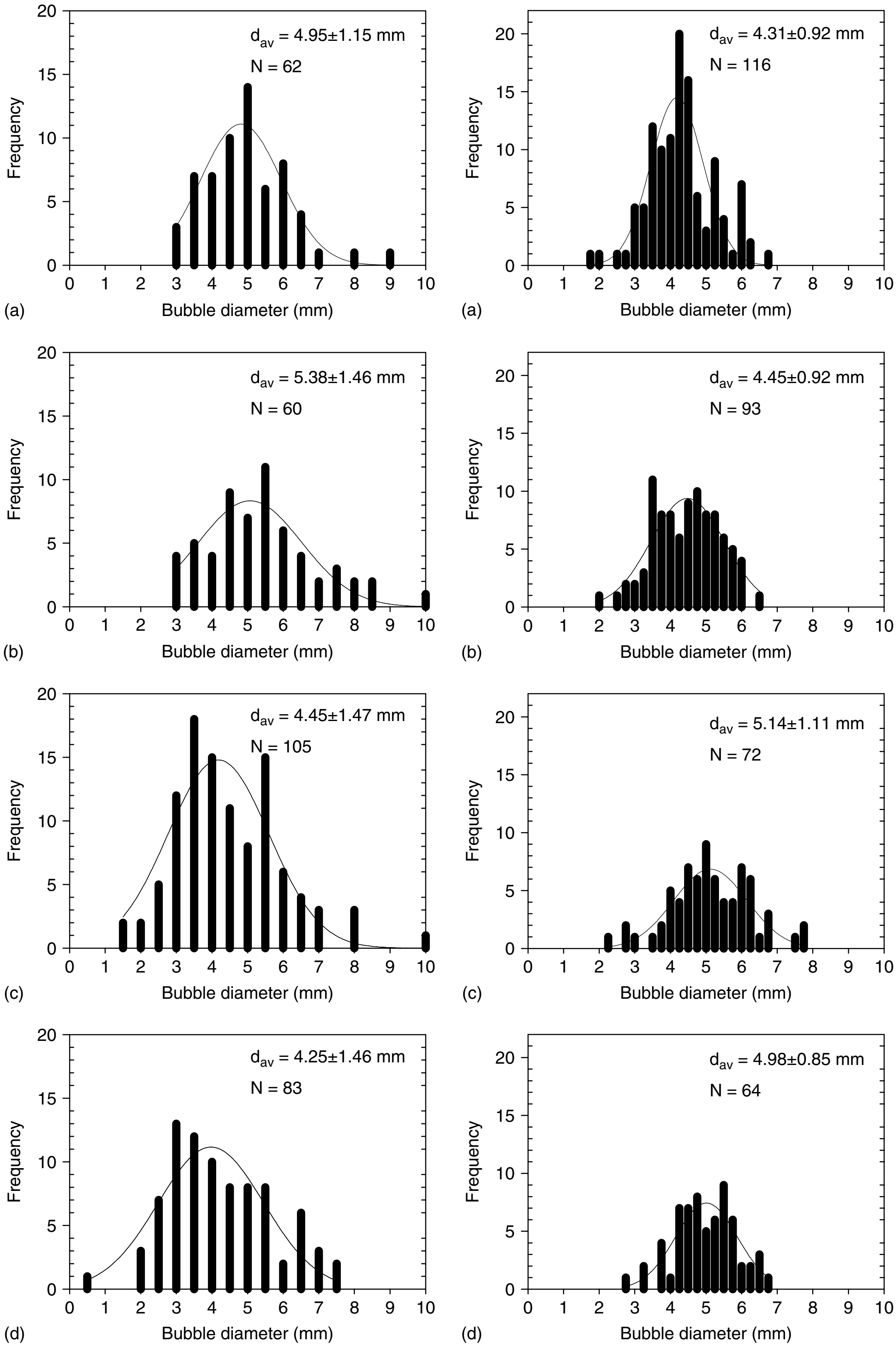


**Figure 2.** Bubble size distribution at a constant liquid flow rate value of 1 $m^3\ h^{-1}$ (left column) and 2 $m^3\ h^{-1}$ (right column). The aeration rate values were as follows: $1.3 \times 10^{-4}\ m^3\ s^{-1}$ (a); $1.8 \times 10^{-4}\ m^3\ s^{-1}$ (b); $3.4 \times 10^{-4}\ m^3\ s^{-1}$ (c); $4.5 \times 10^{-4}\ m^3\ s^{-1}$ (d). Solid lines correspond to best fit normal distributions; $N$ is the number of bubbles measured. Average diameter ($d_{av}$) and standard deviation values are shown based on the normal distribution curves.

size have commonly been reported.[13] In bimodal distributions, the frequency of occurrence of bubbles of the smaller average size is generally much greater than the frequency of occurrence of bubbles of the larger size. In the present work, because of forced circulation of liquid a heterogeneous flow regime was not observed over the entire range of operation.

In conventional bubble columns operated batchwise with respect to liquid, bubble size distribution is known to vary radially at any given axial location.[13]

Axisymmetric size distributions have been reported in the radial direction. In such columns, gas–liquid dispersion flows upward in an axial core zone, but downward flow occurs adjacent to the column walls. In contrast, in forced circulation loops as used here, gas–liquid dispersion flows in the same direction over the entire cross-section of the riser or downcomer zone. This difference is likely to affect bubble size distribution in forced circulation flow across the cross-section of the flow channel. Bubble size distributions in the axial upflow zone of bubble columns have been approximated as Gaussian,[13] but bimodal distributions occur near the walls[13]. Size distributions can vary depending on whether the dispersion is flowing upwards or downwards. For example, in downflow bubble columns, the bubble size distribution has been reported to be log normal[14] instead of the normal distribution observed in the riser zone of the forced circulation reactor used here. Size distributions in the downcomer zone were not investigated.

Although bubble size and size distribution are known to influence gas holdup, gas–liquid mass transfer and liquid phase mixing in gas–liquid contactors, empirical correlations for gas holdup, volumetric mass transfer coefficient, mixing time and liquid phase dispersion coefficients have invariably disregarded size distributions for the sake of simplicity. A bubble size distribution and average size are outcomes of the underlying phenomena of bubble coalescence and breakup. In bubble columns, models have been proposed for estimating bubble size distribution and evolution of size distribution with height.[12,15] but this aspect remains to be investigated for forced circulation loop reactors in which the aeration rate and forced liquid flow rate can be varied independently.

## CONCLUSIONS

Bubble size distribution in the riser zone of a forced circulation loop reactor is satisfactorily approximated as a normal distribution irrespective of the combinations of gas and liquid flow rates used. The Sauter mean bubble size generally declines with increasing liquid flow rate. Increasing gas flow rate at a constant liquid flow rate can positively or negatively influence the median bubble size, depending on the value of the liquid flow rate used.

## REFERENCES

1 Shah YT, Kelkar BG, Godbole and Deckwer WD, Design parameters estimations for bubble column reactors. *AIChE J* **28**:353–379 (1982).
2 Chisti MY, *Airlift Bioreactors*. Elsevier, New York (1989).
3 Sotiriadis AA, Thorpe RB and Smith JM, Bubble size and mass transfer characteristics of sparged downwards two-phase flow. *Chem Eng Sci* **60**:5917–5929 (2005).
4 Marrucci G and Nicodemo L, Coalescence of gas bubbles in aqueous solutions of inorganic electrolytes. *Chem Eng Sci* **22**:1257–1265 (1967).
5 Keitel G and Onken U, Inhibition of bubble coalescence by solutes in air/water dispersions. *Chem Eng Sci* **37**:1635–1638 (1982).
6 Tung HL, Tu CC, Chang YY and Wu WT, Bubble characteristics and mass transfer in an airlift reactor with multiple net draft tube. *Bioprocess Eng* **18**:323–328 (1998).
7 Chisti Y and Moo-Young M, Improve the performance of airlift reactors, *Chem Eng Progress* **89**(6):38–45 (1993).
8 Fadavi A. Circulation reactor, Patent application SK4135U, Industrial Property Office of Slovak Republic (2004).
9 Fadavi A and Chisti Y, Gas–liquid mass transfer in a novel forced circulation loop reactor. *Chem Eng J* **112**:73–80 (2005).
10 Vasconcelos JMT, Rodrigues JML, Orvalho SCP, Alves SS, Mendes RL and Reis A, Effect of contaminants on mass transfer coefficients in bubble column and airlift contactors. *Chem Eng Sci* **58**:1431–1440 (2003).
11 Chisti Y, Pneumatically agitated bioreactors in industrial and environmental bioprocessing: Hydrodynamics, hydraulics and transport phenomena. *Appl Mech Rev* **51**:33–112 (1998).
12 Colella D, Vinci D, Bagatin R, Masi M and Bakr EA, A study on coalescence and breakage mechanisms in three different bubble columns. *Chem Eng Sci* **54**:4767–4777 (1999).
13 Kulkarni AA, Joshi JB and Ramkrishna D, Determination of bubble size distributions in bubble columns using LDA. *AIChE J* **50**:3068–3084 (2004).
14 Mandal A, Kundu G and Mukherjee D, A comparative study of gas holdup, bubble size distribution and interfacial area in a downflow bubble column. *ChERD* **83A**:423–428 (2005).
15 Bordel S, Mato R and Villaverde S, Modeling of the evolution with length of bubble size distributions in bubble columns. *Chem Eng Sci* **61**:3663–3673 (2006).


*J Chem Technol Biotechnol* **83**:105–108 (2008)
DOI: 10.1002/jctb